Journal of Environmental Management 100 (2012) 1–9

Contents lists available at SciVerse ScienceDirect

Journal of Environmental Management

journal homepage: www.elsevier.com/locate/jenvman

The role of Fe(III) modified montmorillonite on fluoride mobility: Adsorption experiments and competition with phosphate

Gonzalo Bia [c], Carlos P. De Pauli [b], Laura Borgnino [a,b,*]

[a] CICTERRA-CONICET, Facultad de Ciencias Químicas, Universidad Nacional de Córdoba, Ciudad Universitaria, 5000 Córdoba, Argentina
[b] INFIQC-CONICET, Facultad de Ciencias Químicas, Universidad Nacional de Córdoba, Ciudad Universitaria, 5000 Córdoba, Argentina
[c] Facultad de Ciencias Químicas, Universidad Nacional de Córdoba, Ciudad Universitaria, 5000 Córdoba, Argentina

ARTICLE INFO

Article history:
Received 19 July 2011
Received in revised form
27 December 2011
Accepted 14 January 2012
Available online

Keywords:
Fluoride
Phosphate
Competitive adsorption
Fe(III)-montmorillonite

ABSTRACT

Fluoride adsorption onto Fe(III) modified montmorillonite was investigated using batch experiments. The effect of reaction time, pH, ionic strength and phosphate, as a competitive anion, was evaluated. Kinetics indicated that adsorption obeys a pseudo-first-order rate law which involves two steps. The fast one (bulk transport/surface reaction) occurs instantaneously. The slower (diffusion in pores) takes hours to complete. The adsorption rate increases by increasing the fluoride concentration and by decreasing pH. The presence of phosphate reduces fluoride adsorption and reveals that both ions are in competition for surface sites. The reduction in fluoride adsorption when phosphate is present depends on the order of adsorbate addition. The higher fluoride adsorption occurs when both anions are added simultaneously, whereas when either fluoride or phosphate is added first, the fluoride adsorption is lower. The presence of fluoride does not have a measurable effect on phosphate adsorption. The results obtained contribute to our understanding of the mobility of fluoride in surface water which has naturally high levels of fluoride, in both the presence and absence of phosphate.

1. Introduction

In relation to human health, fluoride in drinking water has a narrow beneficial concentration range. A low amount ingested in water is usually considered helpful in the prevention of dental cavities, particularly among children (Sujana et al., 1998). In contrast, an excessive amount ingested in drinking water can lead to various diseases (Mohapatra et al., 2009); fluorosis being the most common symptom of high fluoride ingestion. A fluoride concentration of about 0.6–1.2 mg L^{-1} in drinking water can cause dental fluorosis (WHO, 2004). This range varies according to factors such as weather. In temperate climates, symptoms of dental fluorosis do not appear, even when the drinking water contains fluoride concentrations between 1.5 and 2.0 mg L^{-1}; in hot climates, however, where water consumption per day is greater, the disease can occur at much lower concentrations (Cao and Li, 1992; WHO, 2003). The maximum concentration of fluoride permitted in drinking water for human consumption is 1.5 mg L^{-1} (WHO, 2003).

Fluoride contamination in surface water and groundwater arises both from natural and from anthropogenic activities (Camargo, 2003). It is found in plants, soil, and phosphate fertilizers (Loganathan et al., 2001). Slow dissolution of fluoride-containing rocks is one of the most common ways that fluoride is released into groundwater (Camargo, 2003). Minerals containing fluoride include fluorite, apatite, cryolite and topaz. Biotite, muscovite and hornblende can also contain high concentrations of fluoride (Deer et al., 1992). In water, inorganic fluorides usually remain in solution (as fluoride ions) under conditions of relatively low pH and hardness as well as in the presence of ion-exchange materials such as bentonite clays and humic acids (Pickering et al., 1988).

While phosphorous is an essential nutrient in aquatic environments, in excess, however, its concentrations cause eutrophication in lakes and reservoirs (Klapper, 1991). The harmful consequences of eutrophication have been historically recognized and numerous studies have been carried out worldwide in order to understand and control this process (Withers and Jarvie, 2008). The geochemical behaviors of phosphate have been the subject of numerous studies in various disciplines (Borgnino et al., 2006a, 2006b; Harvey and Rhue, 2008; Spiteri et al., 2008).

Under certain conditions fluoride and phosphate could be released and then be re-adsorbed, from sediment to water column and vice versa. Usually, both anions could be adsorbed in iron-

---

* Corresponding author. CICTERRA-CONICET, Facultad de Ciencias Químicas, Universidad Nacional de Córdoba, Ciudad Universitaria, 5000 Córdoba, Argentina. Fax: +54 351 4334188.
E-mail address: borgnino@fcq.unc.edu.ar (L. Borgnino).

0301-4797/$ – see front matter © 2012 Elsevier Ltd. All rights reserved.
doi:10.1016/j.jenvman.2012.01.019

containing minerals, as both anions have a relatively strong affinity for metal hydroxides, especially iron and aluminum hydroxides (Antelo et al., 2005; Luengo et al., 2007; Tang et al., 2009a,b). For that reason, during the last decades, a great deal of research has centered on the adsorption capacity of phosphate and fluoride onto different minerals surfaces (Kau et al., 1998; Harrington et al., 2003; Zhu et al., 2004, 2006; Borgnino et al., 2009), since their mobility and bioavailability in natural environments is affected by its adsorption on particulate matter. A few studies have been conducted using Fe hydroxide coating phyllosilicates (Borgnino et al., 2009), although in natural environments, fluoride and phosphate are commonly adsorbed onto Fe hydroxide coatings, but not solely onto pure Fe/Al hydroxides.

Although the adsorption–desorption behavior of fluoride and phosphate onto metal hydroxides, phyllosilicate minerals and soils has been researched (Kau et al., 1998; Loganathan et al., 2001; Antelo et al., 2005; Tang et al., 2009a,b), investigation of the competitive effect of phosphate on fluoride adsorption, and vice versa, remains limited. In this regard, Tang et al. (2009a) and Kumar et al. (2009) investigated the adsorption of fluoride onto granular ferric hydroxide, including the effect of pH, ionic strength, temperature and major co-existing ions. The competitive effect was analyzed in terms of the decreasing adsorption capacity of fluoride in the presence of different competitors (phosphate, chloride, sulfate and carbonate). The competition with other anions, such as arsenate and selenate, was also studied by Tang et al. (2009b), in this case onto activated alumina. On the other hand, Zhu et al. (2007) analyzed the co-sorption and desorption of fluoride and phosphate on soil, and concluded that the presence of phosphate could markedly enhance fluoride adsorption, which could be attributed to the formation of surface (Al,Fe)–F–P precipitation.

This study primarily aims to investigate the adsorption of fluoride onto Fe(III)-montmorillonite and to analyze the competition effect between fluoride and phosphate for Fe(III)-montmorillonite sites. Fluoride adsorption kinetics was conducted under various experimental conditions and the data obtained was then fitted with different kinetic models. In addition, adsorption isotherms were evaluated. For the competition study, a series of experiments were carried out to assess the effects of phosphate concentration and the order of addition of adsorbates on the adsorption of fluoride and phosphate. The results obtained may contribute to our understanding of the mobility and bioavailability of both anions in contaminated aquifers and groundwater resources.

2. Material and methods

All solutions were prepared from analytical reagent grade chemicals and purified water (Milli-Q system).

2.1. Fe(III)-montmorillonite (Fe-M) synthesis and general characterization

The Fe-M sample employed is the same one used in previous research (Borgnino et al., 2009). Briefly, 550 mL of a 0.01 M Fe(III) nitrate solution (pH 3.5) was mixed with 250 mL of a 2.2% Na-M dispersion in water at the same pH with vigorous stirring for 2 h. A NaOH solution was then added drop by drop up to pH 9; the dispersion was stirred for another 3 h. Finally, the solid was washed with water and dried at 60 °C for 3 days. The resulting solid has an iron content of 77.3 mg g^{-1} and a surface area of 567 m^2 g^{-1}, measured by the methylene blue adsorption method (before the modification the surface area of Na-M was 800 m^2 g^{-1}). More than 60% of the total Fe(III) in this sample corresponds to interlayer/sorbed Fe(III) as XRD pattern and Mössbauer spectra indicated. The remaining fraction was already present in Na-M (structural Fe). If some ferrihydrite was formed as an associated phase, it has not been detected in the diffraction pattern (Borgnino et al., 2009). The net surface charge of Fe-M is always negative in the pH range 4.0–9.0, as demonstrated thought electrophoretic mobility measurements (Borgnino et al., 2010).

2.2. Adsorption experiments

2.2.1. Adsorption kinetics

Batch experiments were used to investigate the fluoride kinetics at different pH levels and concentrations. The reaction was carried out in a cylindrical, water-jacketed reaction vessel covered with a cap. Mixing was performed with a magnetic stirrer; during the kinetic adsorption experiments special care was taken to avoid the presence of CO_2, by keeping the Fe-M suspensions in a N_2 atmosphere. The reaction temperature was kept at 25.0 ± 0.5 °C. To obtain the adsorption kinetics of fluoride in the Fe-M sample, known amounts of Fe-M (1 g L^{-1}) were suspended in 0.01 M $NaNO_3$. After 24 h of pre-equilibration, and upon reaching a constant temperature of 25.0 ± 0.25 °C, a well-known volume of a 0.01 M fluoride solution (NaF) prepared in 0.01 M $NaNO_3$ was added, the initial fluoride concentration range thus being 0.105–0.526 mM (2–10 mg L^{-1}). After that, the pH of the suspension was adjusted by the addition of either HNO_3 or NaOH until the desired pH was obtained; this moment was set as the initial time of the kinetic adsorption experiment. At different reaction times, an aliquot was withdrawn, centrifuged at 9000 rpm for 5 min, filtered through a 0.45 μm cellulose membrane filter and the supernatant separated for fluoride analysis. The reaction was studied for 310 min; the pH was continuously checked and kept constant by adding a minute volume of concentrated 0.1 M HNO_3 or NaOH. Measurements were performed in duplicate, and the errors were around 5%.

2.2.2. Adsorption isotherm

Adsorption edges and isotherms were carried out in the same way that kinetics was performed. Briefly, different volumes of the fluoride solution were added to a Fe-M suspension, so that the initial concentration of fluoride varied between 0.27 and 3.70 mM (5–70 mg L^{-1}). Ionic strength of 0.01 M $NaNO_3$ was used and the pH studied was 4.5 and 7.0. For edge isotherm, the selected concentration of fluoride corresponds to the highest concentration used in the kinetic experiments (0.526 mM). A pH range of 3.5–9.0 and different ionic strengths (0.1 and 0.01 M $NaNO_3$) were selected for the adsorption study. For both experiments, after the samples were shaken for 24 h at room temperature (25.0 ± 0.5 °C), the supernatant solutions were analyzed for pH with an Orion glass combined electrode. The tubes were then centrifuged at 9000 rpm for 5 min, the supernatant filtered through a 0.45-μm cellulose membrane filter and finally the supernatant was separated for fluoride analysis. Measurements were performed in duplicate, and the errors were around 5%.

2.2.3. Competitive adsorption experiments

The competition experiments were carried out at pH 4.5 and 7.0. First, the effect of phosphate on fluoride adsorption was analyzed. In this case, the addition of both anions was simultaneous. The initial concentration of fluoride varied between 0.27 and 3.70 mM and volumes of phosphate solution (prepared in 0.01 M $NaNO_3$) were added, so that the two initial concentrations of phosphate evaluated were 0.30 mM and 1.0 mM. The values of the phosphate initial concentration selected correspond to those required to produce low and high saturation adsorption values in isotherm (middle and plateau values) for phosphate adsorption onto Fe-M (Borgnino et al., 2009). Furthermore, different ways of fluoride and phosphate addition were also considered, i.e.: (i) fluoride addition after phosphate, (ii) simultaneous addition of fluoride and phosphate, and (iii) phosphate addition after fluoride. In these experiments, the phosphate concentration evaluated was 0.30 mM. In all cases, the concentration of Fe-M was 1 g L^{-1} and the ionic strength was 0.01 M $NaNO_3$. Once the samples were shaken for 24 h at room temperature (25.0 ± 0.5 °C), the supernatant solutions were analyzed for pH, centrifuged at 9000 rpm for 5 min, filtered through a 0.45 μm cellulose membrane filter, and the supernatant was then separated for fluoride and phosphate analysis.

2.3. *Chemical analysis*

The total fluoride concentration in the supernatant clear solution was measured using an ion-selective electrode (ISE 25) connected to an Orion pH meter. Prior to obtaining fluoride measurement, a volume of ionic adjusting buffer (TISAB) was added to each solution, and after 30 min the fluoride concentrations were determined (TISAB: 58 g NaCl + 57 ml acetic acid + 10 Na–citrate, adjusted to pH 5.2 with 5 M NaOH in a total volume of 1 L). The TISAB solution was used to adjust the ionic strength and pH solution, and to eliminate any interference from high levels of aluminum and iron present in the solution (Shen et al., 2003). The same volume of TISAB was also added to the standard fluoride solutions, thus obtaining a calibration curve.

Phosphate concentrations were measured by the method proposed by Murphy and Riley (Murphy and Riley, 1962) using a UV–VIS spectrophotometer (Shimadzu UV–VIS 1700) equipped with a 1-cm quartz cell.

The phosphate and fluoride adsorbed was calculated from the difference between the initial anion concentration and the concentration that remained in the solution.

3. Results and discussion

3.1. *Batch adsorption kinetics*

Fig. 1a illustrates the results obtained for fluoride adsorption kinetics on Fe-M at pH 4.5 for four different loading conditions. As discussed herein, fluoride adsorption increases with decreasing pH; therefore only data at a pH level of 4.5 was selected, in order to have a relatively high adsorption. The adsorption increased quickly to almost 50–55% within the first 5 min; over 95% of the fluoride adsorption was achieved within 3 h. This equilibrium time seems to differ for similar materials. For instance, Zhu et al. (2006) indicated that 10 min is necessary to achieve fluoride adsorption equilibrium on hydroxyaluminum-montmorillonite, whereas 40 min is required for a granular ferric hydroxide (GFH) (Kumar et al., 2009). Tang et al. (2009a) also found this time to be longer (5 h) for a GFH. A similar result was reported for a siderite (Liu et al., 2009), while for a Fe–Al–Ce trimetal oxide, the recorded time was 10 h (Wu et al., 2007). Despite these differences, the shape of the kinetic curves is similar: the adsorption is fast within the first minutes and then is much slower during the remainder of the experiment, until the equilibration is reached. Our adsorption kinetic data (Fig. 1a) indicated a very fast initial process between $t = 0$ in the first 5 min. After the fifth minute, adsorption takes place at a much slower rate. It is important to note that with our experimental set-up, 5 min was the minimal time required to extract the first sample.

According to the kinetic data obtained from the experiments, pseudo-first-order (Lagergren, 1898), pseudo-second-order (Ho and McKay, 1999) and Elovich's equation (Chien and Clayton, 1980) have all been used to explain the adsorption mechanism. The corresponding equations are shown in Table 1 (see Supplementary Material). A kinetic equation used by Luengo et al. (2007), based on a pseudo-first-order reaction and two-step processes, was also used (eq. (4) in Table 1 of Supplementary Material). For all the models evaluated, the determination coefficient r^2 was applied to determine which of the kinetic models linear forms fit best. Plotting ln $(q_e - q_t)$ against t, a linear function can be obtained and the rate constant, k_1, for the pseudo-first-order model can be calculated. For the pseudo-second-order model a plot t/q_t versus t should give a straight line and q_e and k_2 can be determined from the slope and intercept of the plot. Regarding to the Elovich model, the values of constants α and β can be obtained from the slope and intercept of the straight line plot of q_t versus ln t.

For our kinetic data, r^2, k_1 and k_2 and the adsorption capacity at equilibrium q_e, calculated and experimental, are listed in Table 1 of Supplementary Material. Data indicate that for the model of pseudo-first-order, the rate constant k_1 is relatively low and the

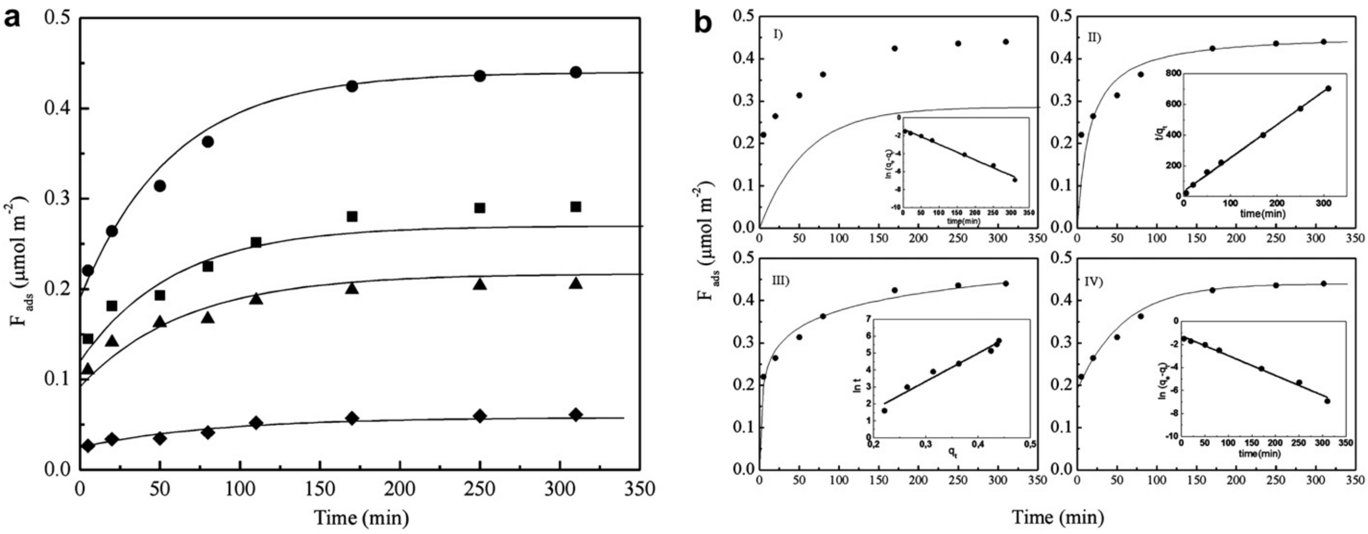

Fig. 1. a) Adsorption kinetics of fluoride onto Fe-M at different initial concentrations: 0.105 mM (diamonds); 0.263 mM (triangles); 0.370 mM (squares); 0.526 mM (solid circles). Solid concentration: 1 g L^{-1}, temperature: 25.0 ± 0.5 °C. Lines show predictions for fluoride adsorption using the two-step pseudo-first-order kinetic model. b) Different kinetic modeling of the adsorption of fluoride onto Fe-M. I) pseudo-first-order kinetic model; II) pseudo-second-order model; III) Elovich model; IV) two-step pseudo-first-order kinetic model. Initial fluoride concentration: 0.526 mM, solid concentration: 1 g L^{-1}, temperature: 25.0 ± 0.5 °C. Insets: linear equation of kinetic models.

determination coefficient is not the highest observed ($r^2 = 0.986–0.993$). The linear fits obtained by applying the pseudo-second-order model with the determination coefficient values ranging from 0.987 to 0.998 indicate that the kinetics behavior can be better approximated to the pseudo-second-order kinetics. For this model the rate constant (k_2) decrease with increasing initial concentrations, which could be attributed to the increased number of fluoride ions available for adsorption (Camacho et al., 2010). Elovich coefficients, α and β, represent the initial rate of adsorption (μmol m^{-2} min^{-1}) and the rate of desorption (μmol m^{-2} min^{-1}), respectively. The behavior observed when the initial concentration increases, is the expected.

As was above mention, according to the r^2 values obtained, the pseudo-second-order model produced a higher determination coefficient for all the initial fluoride concentration, which may imply that the pseudo-second-order model best explains the adsorption process. This approach has been widely used in previous reports (Kumar et al., 2009; Liu et al., 2009; Chen et al., 2010). However, in this study when the nonlinear method was applied to experimental data (using the integrated form of kinetic models), a better analysis was obtained. For our data, the pseudo-second-order reaction (Fig. 1b-II) would suitably fit data for longer times, but would fail in the first data, which is important in determining the initial adsorption rate. On the other hand, Elovich's equation (Fig. 1b-III) seems to fit well with all the data, despite having the lowest r^2 values (Table 1). The pseudo-first-order equation appears to properly represent the shape of the curve; but, as Table 1 (in Supplementary Material) and Fig. 1b-I show, the predicted amounts of fluoride adsorbed are smaller than the experimentally values (by almost half), which would be it suggesting that the adsorption of fluoride does not follow the pseudo-first-order rate mode. Therefore, as noted by Ho (2006), it is inappropriate to use only the determination coefficient r^2 when comparing the best-fitting of the kinetic models. The nonlinear method could be the most effective option to obtain the corresponding kinetic parameters and to deduce the order rate of the process.

As previously stated, the adsorption of fluoride takes place in at least two different processes. The slow process (rate-limiting) is considerably slower than the other and takes hours (or days) to complete. The markedly different time scale of these two processes allows for the assumption that in comparison to the slow process, the fast process is nearly instantaneous. Based on this concept, Luengo et al. (2007) used a pseudo-first-order kinetic model that took into account both processes and focused on the analysis of data in the slow process, for which experimental data is readily available. For our experimental data, this model improves the goodness-of-fit (Fig. 1b-IV). In the initial condition of $t = 0$, the maximum amount of fluoride adsorbed is zero. Afterwards, a significant amount of fluoride was quickly adsorbed during the fast process. This step is represented by the term q_1 in the equation (eq. (4) in Table 1 of Supplementary Material). As reported by Luengo et al. (2007), a factor analogous to $(1 - e^{-kt})$ could be placed by multiplying q_1 in the equation. However, since this process is rapid, its constant rate is assumed to be particularly large, so that the factor is equal to 1. The slow process began with a certain amount of fluoride in surface, which was adsorbed during the fast process. The term $q_2\ (1 - e^{-kt})$ is the amount adsorbed due to the slow process and represents a pseudo-first-order kinetics process in which q_2 is the amount adsorbed due to the slow process and k is the rate constant for this slow process. Thus, the amount adsorbed at the equilibrium ($q_e = q_1 + q_2$) is consistent with that of the experimental data (Fig. 1b-IV). Additionally, although not shown here, the rate of the slow process ($v_{2,0}$) depends linearly on the amount of fluoride adsorbed during the fast process ($r^2 = 0.999$, $p < 0.001$). This indicates that the adsorption rate of the slow process is directly related to the amount of fluoride adsorbed during the fast process. The direct correlation between $v_{2,0}$ and q_2 ($r^2 = 0.997$, $p < 0.001$) may also indicate that the slow process is controlled by a pseudo-first-order reaction. Based on these findings, we proposed a pseudo-first-order reaction model involving a two-step process as the main mechanism responsible for fluoride adsorption onto Fe-M.

Sparks (2003) indicated that bulk transport and chemical reactions on the surface are fast processes, while diffusion transport (film diffusion and intraparticle diffusion) are slow processes, and thus rate-limiting steps. Many authors (Kumar et al., 2009; Liu et al., 2009; Chen et al., 2010) have used the model proposed by Weber and Morris (1962) to identify whether the intraparticle diffusion process is a rate-limiting step. The linear form of intra particle diffusion model is given by

$$q_t = k_{ip}t^{0.5} + C \qquad (1)$$

where C is the intercept, related to the thickness of the boundary layer and k_{ip} is the intraparticle diffusion rate constant. For this model, it is essential that when the intraparticle diffusion is the sole rate-limiting step, a plot of q_t vs $t^{0.5}$ is a straight line passing through the origin. Otherwise, both process simultaneously rate-limit the steps (Weber and Morris, 1962; Liu et al., 2009; Chen et al., 2010). A plot of the quantity of fluoride against the square root of time is shown in Fig. 2. Since the first data obtained with our experimental set-up was at 5 min, the values of fluoride adsorption for $t < 5$ min were estimated from the kinetic model proposed. This data (q_1) was then included in this graph for $0 \leq t < 5$. From this figure, is it clear that the plot is not linear over the entire range of time. The graph reflects three stages, with an initial portion followed by an intermediate linear portion and a plateau. This implies that bulk transport and surface adsorption (stage 1) was very fast, consistent with the analysis previously performed. Then a stage of diffusion transport (stage 2) was attained and maintained for 171 min. Finally, an equilibrium adsorption (stage 3) followed. Therefore, fluoride ions were first quickly transported and adsorbed onto the most readily available adsorption sites, and then were slowly transported and retained by the particles until equilibrium was reached.

Fig. 3 shows the effect of pH on the adsorption kinetics at pH 4.5, 7.0 and 9.0 and 0.526 mM initial fluoride concentration. At a given

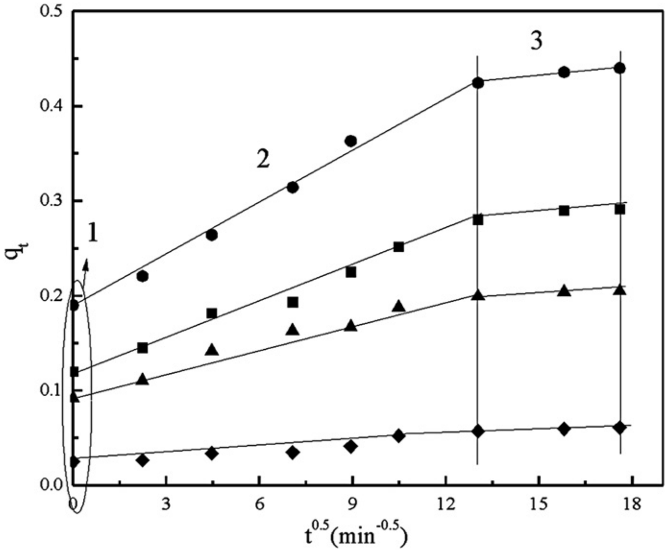

Fig. 2. Intraparticle diffusion kinetic modeling of fluoride adsorption onto Fe-M.

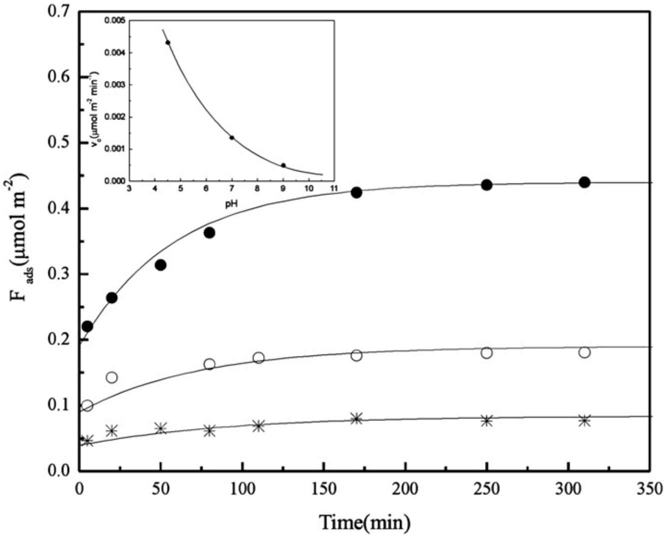

Fig. 3. Kinetic adsorption of fluoride at different pH levels. Initial fluoride concentration 0.526 mM. Solid concentration: 1 g L^{-1}, temperature: 25.0 ± 0.5 °C. Cross: pH 9.0, open circles: pH 7.0, solid circles: pH 4.5. Lines show predictions for fluoride adsorption using the two-step pseudo-first-order kinetic model. Inset: initial kinetic rates for pH 4.5, 7.0 and 9.0.

time, the adsorption increases as the pH decreases. The values of q_1 and q_2 obtained with the kinetic model proposed also increase as the pH decreases, suggesting that the pH affects both processes. The adsorption rates of the slow process ($v_{2,0}$), which were also obtained with the kinetic model, depend on the pH decreasing rapidly as pH increases from 4.5 to 7.0 and more slowly from 7.0 to 9.0 (inset Fig. 3).

3.2. *Effect of pH and ionic strength*

The effect of pH and ionic strength on fluoride adsorption was examined (Fig. 4). Fluoride adsorption increases from pH 5.0 to 3.7. Between 5.0 and 7.0 the adsorption is almost constant, while for a pH higher than 7.0, a slight decrease in fluoride adsorption is observed. Because HF is weakly ionized in solution at low pH values (p*K*a = 3.2), the corresponding uptake of fluoride is reduced at an acidic pH, and consequently a fraction of the fluoride becomes unavailable for adsorption. Our experimental minimum pH condition was 3.5, so this pH may be close to the higher pH adsorption value. The fact that fluoride adsorbs significantly onto the net negative surface of Fe-M (Borgnino et al., 2010) indicates that adsorption is not driven by electrostatic interactions. The net electrostatic repulsion between Fe-M and fluoride appears to be overcome by some kind of specific interaction, such as the formation of inner-sphere surface complexes between fluoride and Fe(III) species. This type of interaction can be evaluated by the effect of ionic strength on the adsorption process. Fig. 4 shows that no salt effect is found in fluoride adsorption, supporting the premise that an inner-sphere surface complex may be present (Stumm and Morgan, 1996). The small decrease in the adsorption of fluoride at low pH and high ionic strength may be only a consequence of aggregation of Fe-M particles. This process, which is more favorable at low pH, could block some sites of Fe-M edges involved in the adsorption of fluoride. Therefore, adsorption can be explained as a mechanism of a ligand-exchange reaction, where fluoride ions are exchanged against OH$^-$ ions (Hiemstra and Van Riemsdijk, 2000). The effect of pH on fluoride adsorption is likewise a consequence of both the specific binding of fluoride ions onto Fe-M surface groups and the electrostatic repulsion; at low and intermediate pH, adsorption is more favorable because the edge Fe-M surface sites are positively charged, promoting the specific interaction. At a high pH, surface sites and fluoride ions are negatively charged and, although adsorption occurs, the electrostatic repulsion between fluoride ions and negatively charged sites increases. As a result the fluoride adsorption decreases.

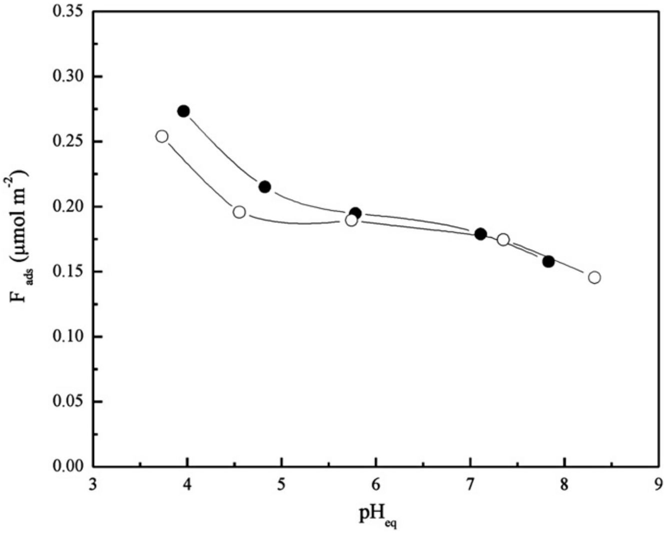

Fig. 4. Effect of ionic strength on fluoride adsorption. Open circles: 0.1 M $NaNO_3$, solid circles: 0.01 M $NaNO_3$.

3.3. *Fluoride adsorption and phosphate competition*

Adsorption can be explained based on a number of theoretical models, where Langmuir and Freundlich models are the most used. Its mathematical form is written as:

$$\frac{C_e}{q_e} = \frac{C_e}{q_{max}} + \frac{1}{q_{max}K_L} \tag{2}$$

where q_{max} is the maximum adsorption capacity corresponding to complete monolayer coverage (μmol m^{-2}) and K_L is a constant indirectly related to adsorption capacity and energy of adsorption which characterizes the affinity of the adsorbate with the adsorbent. A straight line is obtained when C_e/q_e was plotted against C_e and q_{max}, and K_L could be calculated from the slopes and intercepts. The equation for Freundlich model is commonly represented by

$$\ln q_e = \ln K_f + \frac{1}{n}\ln C_e \tag{3}$$

where K_f and n are the Freundlich constants characteristics of the system, indicating the adsorption capacity and the heterogeneity of the adsorbent, respectively. From the slope and intercept of the straight portion of the linear plot obtained by plotting ln q_e against ln C_e the values of Freundlich parameters were calculated.

Fig. 5 shows isotherm for fluoride adsorption onto Fe-M at pH 4.5 and 7.0. As the competition between fluoride and phosphate was also studied, the corresponding isotherm for phosphate at the same pH has been included in the figure for comparative purposes (inset Fig. 5). The Langmuir and Freundlich models were used to estimate the parameters of adsorption (see Table 2 in Supplementary Material). Table 2 shows that the Langmuir isotherm model has higher determination coefficients r^2 (>0.978) indicating that the Langmuir model fits the experimental data well. The Langmuir model supposes that uptake of ions occurs on a homogenous surface by monolayer adsorption without any

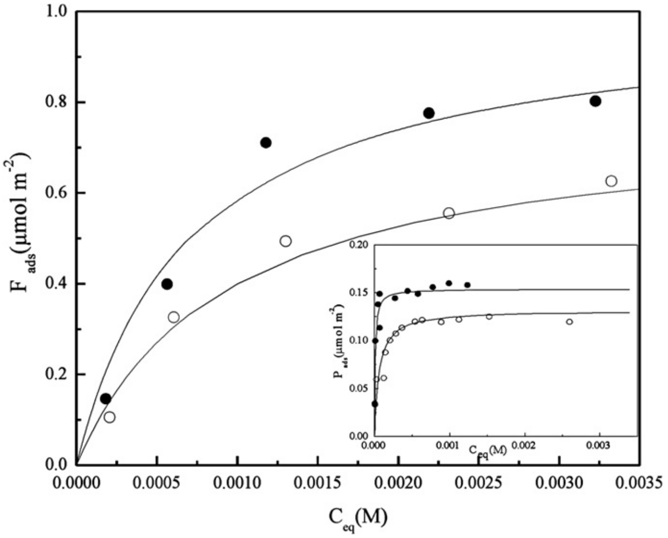

Fig. 5. Fluoride adsorption isotherms onto Fe-M. Solid circles: pH 4.5; open circles pH: 7.0. Inset: phosphate adsorption isotherms on Fe-M. Solid circles: pH 4.5; open circles: pH 7.0. Lines represent the fit by the Langmuir equation.

interaction between adsorbed ions, with homogeneous binding sites, equivalent sorption energies, and no interaction between adsorbed species. It is important to mention that, although the Langmuir model fits the experimental data does not mean that the adsorption of fluoride and phosphate onto Fe-M takes place according with the conditions established by the model. Despite this, data obtained with the models (K, q_{max}) can be useful for comparative purposes of the adsorption behavior.

The fluoride adsorption increases as the pH decrease (Fig. 5) and the corresponding values of q_{max} estimated using Langmuir approach are 0.90 and 0.76 μmol m^{-2} for pH 4.5 and 7.0, respectively. Two important results can be derived from Fig. 5: i) the fluoride q_{max} values obtained are much higher than those corresponding to phosphate (see also Table 2 in Supplementary Material); and ii) the affinity of phosphate for the Fe-M surface is really stronger than for fluoride ions (Table 2 in Supplementary Material). The higher fluoride adsorption capacity may be a consequence of the small fluoride ion size that phosphate shows (fluoride = 0.133 nm; phosphate = 0.22 nm). As a consequence the fluoride can more easily diffuse into pores than phosphate is able to. Additionally, as noted previously, fluoride forms inner-sphere surface complexes with OH^- groups and the main complex involved is the single coordinated surface complex. In contrast to fluoride, phosphate may form a monodentate and a bidentate surface complex. Borgnino et al. (2010) found that nonprotonated bidentate ($(FeO)_2PO_2$) and monoprotonated bidentate ($(FeO)_2OHPO$ were the main surface complexes at pH 4.5, while nonprotonated bidentate and nonprotonatedmonodentate ($(FeO)_2PO_2$ or $(FeO)PO_3{-}H$) and $(FeO)PO_3$) were the surface complexes at pH 7.0 and 9.0. This means that when a bidentate surface complex is formed, phosphate anions occupy (or block) more surface sites than fluoride. As a result, for the same initial surface conditions and initial anion concentration, the maximum amount of phosphate adsorbed is lower in relation to that obtained with fluoride ions.

3.3.1. *The effect of phosphate on fluoride adsorption: pH and different initial phosphate concentrations*

Fig. 6a shows the fluoride isotherm for pH 4.5 and 7.0 in the presence and absence of two initial phosphate concentrations, and in simultaneous addition of both anions. The adsorption values obtained, for phosphate or fluoride were compared with the isotherm adsorption values reached in the absence of the competitor. For fluoride adsorption at both pH levels, the adsorption decreases as the concentration of phosphate increases. This suggests that because of the above-described adsorption mechanism, a competition adsorption process between fluoride and phosphate occurs. Electrostatics may also play a role in the competition. Since both anions are negatively charged, an increase in the phosphate concentration may also increase the negative electrical potential near the Fe-M interface. Therefore, the overall affinity of fluoride anions for the surface should be decreased and its adsorption reduced. In addition to competition and some electrostatic effect, the larger size of the phosphate anion may block part of the surface when it is adsorbed, decreasing the ability of fluoride anions for diffusing into pores. With regards the pH effect, at a lower pH the competition is stronger than at higher levels. At pH 4.5, phosphate reduces fluoride adsorption by 80%, while at pH 7.0 its reduction of fluoride is 58% (at the highest phosphate concentration in both cases). This result is expected because more phosphate is adsorbed at a lower pH (Borgnino et al., 2010). In addition, consistent with the explanation above, phosphate forms bidentate surface complexes at pH 4.5 and 7.0, although the monodentate is also formed at pH 7.0. As a consequence, to adsorb phosphate as a bidentate complex, more surface sites are occupied by phosphate, while fewer are available for fluoride and a larger decrease in fluoride adsorption is detected at pH 4.5.

Fig. 6b shows the effect of fluoride on phosphate adsorption. For pH 4.5 and 7.0 at the two initial phosphate concentrations evaluated, there is a slightly decrease in the adsorption of phosphate with the increase of fluoride concentration in the solution. In addition, the amount of phosphate adsorbed is similar to that which is obtained in the absence of fluoride for both initial phosphate concentrations at pH 7.0, but only for low phosphate concentration (0.30 mM) at pH 4.5. This behavior reflects the greater phosphate surface affinity for Fe-M, because it is adsorbed in its maximum adsorption capacity despite the competition of the fluoride. However, at a pH of 4.5 along with a high phosphate initial concentration (1.0 mM), the values of adsorbed phosphate are lower than those which are achieved in the absence of fluoride (0.03 μmol m^{-2} instead of 0.16 μmol m^{-2}). In this case, the initial phosphate concentration is higher and both ions must compete simultaneously for common sites. The adsorption process probably still requires extra time to approach equilibrium. The experiment was run for 72 h and the phosphate adsorption increased in ~3 times; however, it failed to reach the equilibrium value obtained in the absence of fluoride.

3.3.2. *The effect of phosphate on fluoride adsorption: order of addition*

In the environment, it is likely that fluoride and phosphate are sequentially introduced and accumulate into soil or sediment. The different methods of addition may lead to different impacts on phosphate and fluoride adsorption. Fig. 7a and b show the effects of phosphate addition on fluoride adsorption at pH 4.5 and 7.0, at an initial phosphate concentration of 0.30 mM. The reduction in fluoride adsorption varies depending on the order of the addition of adsorbates. For example, when fluoride is added at the beginning of the experiment (F + P), the subsequent addition of phosphate induces its adsorption, and phosphate must be adsorbed by displacing some previously adsorbed fluoride ions. The amount of phosphate adsorbed (Fig. 7c and d) coincides with phosphate adsorption in the absence of fluoride, but the fluoride adsorbed largely decreases (77% for pH 4.5 and 67% for pH 7.0), in relation to the case of fluoride alone. When phosphate is added first (P + F), fluoride appears not to be able to displace the phosphate ions

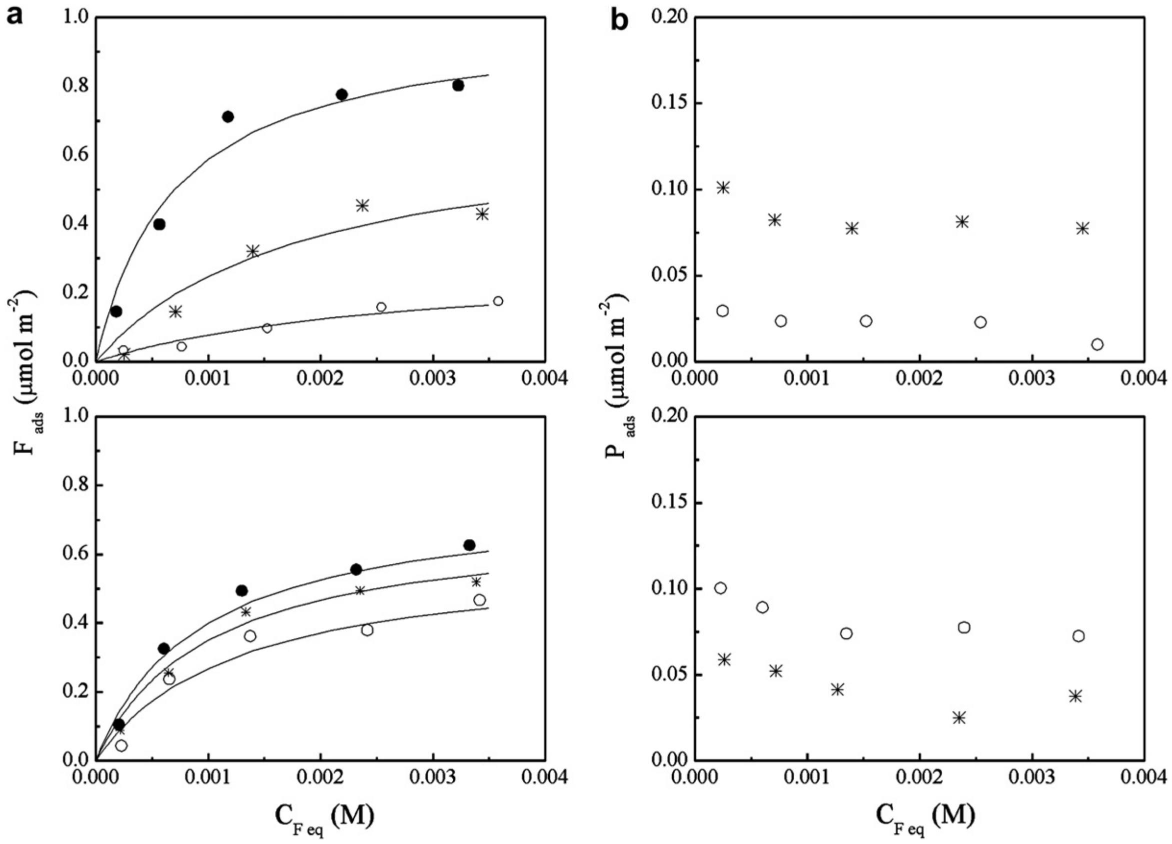

Fig. 6. a) Fluoride adsorption isotherm for pH 4.5 (top) and 7.0 (down) in the presence and absence of phosphate. Solid circles: in absence; cross: 0.3 mM of phosphate; open circles: 1.0 mM of phosphate. b) Influence of fluoride on phosphate adsorption on Fe-M for pH 4.5 (top) and 7.0 (down). Cross: 0.3 mM of phosphate; open circles: 1.0 mM of phosphate. Lines represent the fit by the Langmuir equation.

which have been previously adsorbed, as the amount of phosphate adsorbed closely coincides with those obtained in the absence of fluoride (Fig. 7c and d). In this case, a further decrease in fluoride adsorption (Fig. 7a and b) may be produced by the fact that the previously adsorbed phosphate blocks some surface pores, thereby preventing fluoride diffusion into the pores. In contrast, the simultaneous addition and adsorption of both adsorbates (F and P) suggests that fluoride and phosphate should be adsorbed simultaneously at the Fe-M surface and should compete for common sites. In this case, the reduction in fluoride adsorption is lower than in the other cases. This behavior can be related to the type of surface complex that phosphate develops with Fe-M surface sites. When both adsorbates are simultaneously added, an increase in the negative electrical potential near the interface is expected. As a result, the fluoride is adsorbed by a single coordination with hydroxyl anions; but the phosphate should be adsorbed as a monodentate surface complex (rather than its bidentate form that usually form at pH 4.5 and 7.0). This change in the phosphate adsorption mode is a response to the fact that when the monodentate surface complex is developed, the negative charge of the phosphate ion is further from the negative surface charge of Fe-M, and thus the electrostatic repulsion is reduced and adsorption occurs (Hiemstra and Van Riemsdijk, 1999). This disposition of phosphate ions on the surface allows for a greater number of surface sites available to adsorb fluoride (and phosphate simultaneously), so the quantity of fluoride adsorbed is higher than when obtained through the other manners of addition. In contrast, when phosphate (or fluoride) is added first, there is no competition between the anions for the surface sites. Consequently, the surface phosphate complex favored at pH 4.5 and 7.0 is the bidentate form, although the monodentate should also be present at pH 7.0 (Borgnino et al., 2010). Therefore, more surface sites would be occupied by adsorbed phosphate, and fewer sites would be available for fluoride adsorption (at least half), hence a larger decrease in fluoride adsorption can be observed. In each these examples, the phosphate adsorption is similar (Fig. 7c and d) and coincides with the values obtained in the phosphate isotherm in the absence of a competitor. This is a consequence of the stronger affinity of phosphate, producing a preferential adsorption even when fluoride is present.

The difference in fluoride adsorption observed when the order of addition is varied may also be due to the fact that equilibrium may not always be achieved under the conditions studied. When both anions are added simultaneously, equilibrium seems to be reached, and thus the higher value of fluoride adsorption is observed. However, when one of the anions is added first, equilibrium would probably not be achieved due to the slower desorption rate of the anion previously adsorbed, especially when the phosphate is added first. Antelo et al. (2007) found similar results for humic acid adsorption on goethite and its competitive interaction with phosphate.

3.4. Environmental implications

The findings presented here are of important significance to understanding the mobility of fluoride in water with elevated natural levels of fluoride, in both the presence and absence of phosphate. First, fluoride could be adsorbed onto Fe-M in the pH range of surface water and groundwater (pH range 6–8), and its adsorption is higher than previous values reported for individual

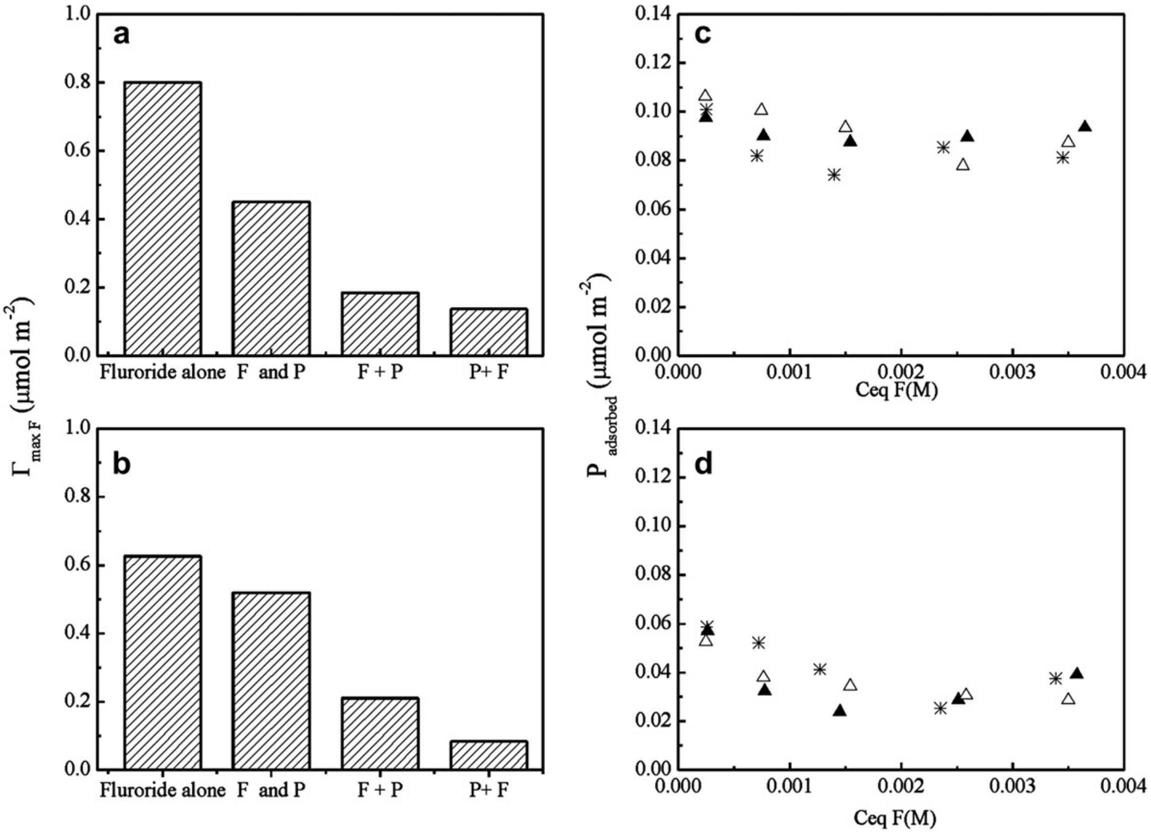

Fig. 7. Effect of the order of addition of the adsorbates on fluoride adsorption: a) pH 4.5 and b) 7.0. The values plotted correspond to Γ_{max} adsorption values for fluoride adsorption in the absence and presence of initial phosphate concentration of 0.3 mM. Influence of fluoride on phosphate adsorption on Fe-M: c) pH 4.5 and d) pH 7.0 for different adsorbate addition orders. Cross: simultaneous; solid triangles: fluoride first; open triangles: phosphate first.

sediment component minerals such as GFH (Tang et al., 2009a; Kumar et al., 2009), kaolinite (Kau et al., 1997), alumina (Tang et al., 2009b) and bentonite (Kau et al., 1997), but slightly lower than for hydroxyaluminum-montmorillonite (Zhu et al., 2006). This indicates that although the weathering of fluoride minerals may act as an internal continuous source of fluoride, the presence of clay minerals coated with Fe hydroxides (in the silt-size fraction of sediments) can retain fluoride through its adsorption, which reduces their mobility and, therefore, its bioavailability in aquatic environments. On the other hand, the presence of phosphate reduces its adsorption. This behavior would suggest that, in situations where both ions are present at the same time (e.g.: eutrophic environments whose sediments have a composition rich in fluoride minerals), phosphate is preferentially retained in the solid phase while fluoride decreases its adsorption; so its movility and bioavailability is enhanced.

4. Conclusions

The study of fluoride adsorption and its competition with phosphate is valuable in understanding the movement of these species in the environment. Fluoride adsorption obeys a pseudo-first-order rate law consisting of two steps: the fast step that arises almost instantaneously in the first minutes, and the slow step that takes hours or days to complete. Bulk transport and surface reaction are involved in the fast process, while the slow process is controlled by the diffusion in pores. The adsorption rate increases by increasing the fluoride concentration and by decreasing the pH.

Comparing the individual fluoride and phosphate adsorption capacities onto Fe-M, fluoride adsorbs more than phosphate; however, the former has a stronger surface affinity. Regarding competition, data for fluoride and phosphate adsorption onto Fe-M reveals that both adsorbates compete for common surface sites. The presence of phosphate reduces fluoride adsorption and decreases as phosphate concentration increases. Additionally, this reduction depends on the order of adsorbate addition. The higher fluoride adsorption occurs when both anions are added simultaneously, whereas when either the fluoride or phosphate is added first, the fluoride adsorption is lower. The type of surface complex that phosphate forms with surface sites and/or extra time needed to reach complete equilibrium explains the difference in fluoride adsorption when the order of addition is varied. The presence of fluoride has no measurable effect on phosphate adsorption.

Acknowledgments

This work was financed by Argentina's FONCYT, SECYT-UNC and CONICET. L. Borgnino and C. P. De Pauli, are members of CICyT in Argentina's CONICET. Language assistance by native English speaker Wendy Walker is gratefully acknowledged.

Appendix. Supplementary material

Supplementary data associated with this article can be found, in the online version, at doi:10.1016/j.jenvman.2012.01.019.

References

Antelo, J., Avena, M., Fiol, S., Lopez, R., Arce, F., 2005. Effect of phosphate and ionic strength on the adsorption of phosphate and arsenate at the goethite-water interface. J. Colloid Interface Sci. 285, 476–486.

Antelo, J., Arce, F., Avena, M., Fiol, S., López, R., Macías, F., 2007. Adsorption of a soil humic acid at the surface of goethite and its competitive interaction with phosphate. Geoderma 138, 12–19.

Borgnino, L., Orona, C., Avena, M., Maine, A., Rodríguez, A., De Pauli, C.P., 2006a. Phosphate concentration an association as revealed by sequential extraction and microprobe analysis: the case of two Argentinean reservoirs. Water Resour. Res. 42, W01414. doi: 101029/2005WR004031.

Borgnino, L., Avena, M., De Pauli, C.P., 2006b. Surface properties of sediments from two Argentinean reservoirs and the rate of phosphate release. Water Res. 40, 2659–2666.

Borgnino, L., Avena, M.J., De Pauli, C.P., 2009. Synthesis and characterization of Fe(III)-montmorillonites for phosphate adsorption. Colloid. Surface. A 341, 46–52.

Borgnino, L., Giacomelli, C.E., Avena, M.J., De Pauli, C.P., 2010. Phosphate adsorbed on Fe(III) modified montmorillonite: surface complexation by ATR-FTIR spectroscopy. Colloid. Surface. A 353, 238–244.

Camacho, L.M., Torres, T., Saha, D., Deng, S., 2010. Adsorption equilibrium and kinetics of fluoride on sol–gel-derived activated alumina adsorbents. J. Colloid Interface Sci. 349, 307–313.

Camargo, J.A., 2003. Fluoride toxicity to aquatic organisms: a review. Chemosphere 50, 251–264.

Cao, S.R., Li, Y.F., 1992. The evaluation of indoor air quality in areas of endemic fluorosis caused by coal combustion. In: Proceedings of the XIX Conference of the International Society for Fluoride Research. Department of Hygiene and Public Health, Osaka Medical College, Kyoto, Japan, p. 38.

Chen, N., Zhang, Z., Feng, C., Sugiura, N., Li, M., Chen, R., 2010. Fluoride removal from water by granular ceramic adsorption. J. Colloid Interface Sci. 348, 579–584.

Chien, S.H., Clayton, W.R., 1980. Application of Elovich equation to the kinetics of phosphate release and sorption in soils. Soil Sci. Soc. Am. J. 44, 265–268.

Deer, W.A., Howie, R.A., Zussman, J., 1992. An Introduction to the Rock Forming Minerals, second ed. Longman, Hong Kong.

Harrington, L.F., Cooper, E.M., Vasudevan, D., 2003. Fluoride sorption and associated aluminum release in variable charge soil. J. Colloid Interface Sci. 267, 302–313.

Harvey, O.R., Rhue, R.D., 2008. Kinetics and energetic of phosphate sorption in a multicomponent Al(III)–Fe(III) hydr(oxide) sorbent system. J. Colloid Interface Sci. 322, 384–393.

Hiemstra, T., Van Riemsdijk, W.H., 1999. Surface structural ion adsorption modeling of competitive binding of oxyanions by metal (hydr)oxides. J. Colloid Interface Sci. 210, 182–193.

Hiemstra, T., Van Riemsdijk, W.H., 2000. Fluoride adsorption on goethite in relation to different types of surface sites. J. Colloid Interface Sci. 225, 94–104.

Ho, Y.-S., 2006. Second-order kinetic model for the sorption of cadmium onto tree fern: a comparison of linear and non-linear methods. Water Res. 40, 119–125.

Ho, Y.S., McKay, G., 1999. Pseudo-second-order model for sorption processes. Process Biochem. 34, 451–465.

Kau, P.M.H., Smith, D.W., Binning, P., 1997. Fluoride retention by kaolin clay. J. Contam. Hydrol. 28, 267–288.

Kau, P.M.H., Smith, D.W., Binning, P., 1998. Experimental sorption of fluoride by kaolinite and bentonite. Geoderma 84, 89–108.

Klapper, H., 1991. Control of Eutrophication in Inland Waters. Ellis Horwood, Chichester.

Kumar, E., Bhatnagar, A., Ji, M., Jung, W., Lee, S.-H., Kim, S.-J., Lee, G., Song, H., Choi, J.-Y., Yang, J.-S., Jeon, B.-H., 2009. Defluoridation from aqueous solutions by granular ferric hydroxide (GFH). Water Res. 43, 490–498.

Lagergren, S., 1898. About the theory of so-called adsorption of soluble substances. K. Svenska Vetenskapsakad. Handl. 24, 1–39.

Liu, Q., Guo, H.M., Shan, Y., 2009. Adsorption of fluoride on synthetic siderite from aqueous solution. J. Fluor. Chem. 131, 635–641.

Loganathan, P., Hedley, M.J., Wallace, G.C., Roberts, A.H.C., 2001. Fluoride accumulation in pasture forages and soils following long-term applications of phosphorus fertilizers. Environ. Pollut. 115, 275–282.

Luengo, C., Brigante, M., Avena, M., 2007. Adsorption kinetics of phosphate and arsenate on goethite: a comparative study. J. Colloid Interface Sci. 311, 354–360.

Mohapatra, M., Anand, S., Mishra, B.K., Giles, D.E., Singh, P., 2009. Review of fluoride removal from drinking water. J. Environ. Manage. 91, 67–77.

Murphy, J., Riley, J.P., 1962. A modified single solution method for the determination of phosphate in natural waters. Anal. Chim. Acta 27, 31–36.

Pickering, W.F., Slavek, J., Waller, P., 1988. The effect of ion exchange on the solubility of fluoride compounds. Water Air Soil Pollut. 39, 323–336.

Shen, F., Chen, X., Gao, P., Chen, G., 2003. Electrochemical removal of fluoride ions from industrial wastewater. Chem. Eng. Sci. 58, 987–993.

Sparks, D., 2003. Environmental Soil Chemistry, second ed. Academic Press, Amsterdam.

Spiteri, C., Van Cappellen, P., Regnier, P., 2008. Surface complexation effects on phosphate adsorption to ferric iron oxyhydroxides along pH and salinity gradients in estuaries and coastal aquifers. Geochim. Cosmochim. Acta 72, 3431–3445.

Stumm, W., Morgan, J.J., 1996. Aquatic Chemistry, third ed. John Wiley and Sons Inc, New York.

Sujana, M.G., Thakur, R.S., Rao, S.B., 1998. Removal of fluoride from aqueous solution by using alum sludge. J. Colloid Interface Sci. 206, 94–101.

Tang, Y., Guan, X., Wang, J., Gao, N., McPhail, M.R., Chusei, C.C., 2009a. Fluoride adsorption onto granular ferric hydroxide: effect of ionic strength, pH, surface loading, and major co-existing anions. J. Hazard. Mater. 171, 774–779.

Tang, Y., Guan, X., Su, T., Gao, N., Wang, J., 2009b. Fluoride adsorption onto activated alumina: modeling the effects of pH and some competing ions. Colloids Surf. A 337, 33–38.

WHO, 2003. Fluoride in Drinking-water: Background Document for Preparation of WHO Guidelines for Drinking-water Quality. Geneva.

WHO, 2004. Guidelines for Drinking-Water Quality, third ed., vol. 1. Geneva.

Weber, W.J., Morris, J.C., 1962. Advances in water pollution research: removal of biologically – resistant pollutants from waste waters by adsorption. In: Proc. Int. Conf. on Water Pollution Symp 2. Pergamon Press, Oxford, pp. 231–266.

Withers, P.J.A., Jarvie, H.P., 2008. Delivery and cycling of phosphorus in rivers: a review. Sci. Total Environ. 400, 379–395.

Wu, X., Zhang, Y., Dou, X., Yang, M., 2007. Fluoride removal performance of a novel Fe–Al–Ce trimetal oxide adsorbent. Chemosphere 69, 1758–1764.

Zhu, M.-X., Jiang, X., Ji, G.-L., 2004. Interactions between variable charge soils and acidic solutions containing fluoride: an investigation by using repetitive extractions. J. Colloid Interface Sci. 276, 159–166.

Zhu, M.-X., Xie, M., Jiang, X., 2006. Interaction of fluoride with hydroxyaluminum-montmorillonite complexes and implications for fluoride-contaminated acidic soils. Appl. Geochem. 21, 675–683.

Zhu, M.-X., Ding, K.-Y., Jiang, X., Wang, H.-H., 2007. Investigation on co-sorption and desorption of fluoride and phosphate in a red soil of china. Water Air Soil Pollut. 183, 455–465.